

Bartosz Wójtowicz*, Waldemar Pyda

AGH-University of Science and Technology, Faculty of Materials Science and Ceramics, al. Mickiewicza 30, 30-059 Krakow, Poland
*Corresponding author. E-mail: bartosz.wojtowicz@agh.edu.pl

Received (Otrzymano) 06.03.2012

INFLUENCE OF TWO-STEP SINTERING ON MICROSTRUCTURE EVOLUTION AND MECHANICAL PROPERTIES OF ALUMINA-NANOZIRCONIA COMPOSITES

In this work we present the preparation of 2 and 12 vol.% zirconia alumina composites via filter pressing and pressureless sintering at a constant heating rate (CHR), by means of two-step sintering (TSS) and reverse two-step sintering (RTSS). Nanozirconia (10 nm) and microalumina (175 nm) powders were used. The resultant composites were characterized in terms of their microstructural (density, grain size) and mechanical (hardness, fracture toughness) properties. The heating schedule showed an insignificant effect on the density of the composites. TSS produced composites of the best properties and finest microstructure, while RTSS in the case of samples containing 12 vol.% of zirconia, produced the coarsest grains. The resultant densities were close to 95%, but the fracture toughness and hardness were reasonably good: (7.0 ± 0.2) MPa·m^{0.5} and (20.8 ± 0.2) GPa for the TSS sample containing 12 vol.% zirconia, respectively.

Keywords: ZTA, two step sintering, microstructure, mechanical properties, composite

WPŁYW SPIEKANIA DWUETAPOWEGO NA EWOLUCJĘ MIKROSTRUKTURY I WŁAŚCIWOŚCI MECHANICZNE KOMPOZYTÓW TLENEK GLINU-TLENEK CYRKONU

W pracy przedstawiono wytwarzanie kompozytów ZTA (Zirconia Toughened Alumina) zawierających 2 i 12 % obj. tlenku cyrkonu. Kompozyty zostały wytworzone techniką prasowania filtracyjnego i spiekania swobodnego przy zastosowaniu różnych krzywych spiekania: ze stałą szybkością grzania (CHR), w cyklach spiekania dwuetapowego (TSS) oraz odwróconego spiekania dwuetapowego (RTSS). Do wytworzenia kompozytu wykorzystano nanoproszek tlenku cyrkonu o średnim rozmiarze ziaren wynoszącym 10 nm oraz mikroproszek tlenku glinu o średnim rozmiarze ziaren wynoszącym 175 nm. Otrzymane kompozyty były charakteryzowane pod kątem parametrów mikrostruktury (gęstość, rozmiar ziaren) oraz właściwości mechanicznych (twardość, odporność na kruche pękanie). Przebieg krzywej spiekania wykazał nieznaczny wpływ na gęstość próbek. Przy zastosowaniu spiekania dwuetapowego uzyskano najlepsze właściwości i najdrobniejszą mikrostrukturę, podczas gdy zastosowanie odwróconego spiekania dwuetapowego prowadziło do otrzymania kompozytu Al₂O₃ - 12% obj. tlenku cyrkonu o największych ziarnach w spieku. Pomimo stosunkowo niskich gęstości spieków, wynoszących w przybliżeniu 95%, dla kompozytu zawierającego 12% obj. tlenku cyrkonu uzyskano dobre właściwości mechaniczne: twardość wynoszącą $20,8 \pm 0,2$ GPa i odporność na kruche pękanie wynoszącą $7,0 \pm 0,2$ MPa·m^{0,5}.

Słowa kluczowe: ZTA, spiekanie dwuetapowe, mikrostruktura, właściwości mechaniczne, kompozyt

INTRODUCTION

Two step sintering (TSS) was developed by Chen and Wang [1] for effective powder consolidation using pressureless sintering to obtain dense, fine-grained polycrystalline materials. In the first stage of sintering, a low temperature consolidated green sample is heated continuously to a temperature T_1 to obtain a density of 75÷90% of the theoretical density [2]. In the second one, the sample is cooled rapidly to a temperature T_2 for final sintering lasting a few or even over a dozen hours. In such a case, the advantageous difference in kinetics between the grain boundary diffusion responsible for pore shrinkage and grain-boundary migration is generated, which results in a fine, even nano-grained micro-

structure and high density. The TSS method has been applied with success to both oxide and non-oxide one phase ceramics [3-12]. The reported microstructures showed mean grain sizes a few times smaller than the size obtained in the case of continuous rate sintering at the first stage temperature of TSS.

A two-step schedule of low-high temperatures (reverse two-step sintering - RTSS) was also applied to limit grain growth, while maintaining grain boundary diffusion on a reasonable level [10]. The approach utilized the benefits of low-temperature sintering, and was used with success to manufacture crack free, dense monoclinic zirconia monoliths. The mono-

clinic->tetragonal transformation in pure ZrO_2 imposes the limit of sintering temperature and hinders the application of Chen's approach.

Reinforcing composite particles increases the activation energy of the densification of a matrix powder [13, 14], and forces the application of higher T_2 temperatures. Only a few attempts of two-step sintering of composite materials have been reported. Silicon nitride-barium aluminosilicate composite materials with a modified microstructure have been manufactured by this method [15], which increased the bending strength and fracture toughness. However, the hardness of the TSS samples appeared lower than in the case of natural sintering.

Wang *et al.* [16] used two-step sintering in processing a high-density alumina-5 wt% zirconia composite. A small grain size ranging from $0.62 \div 0.88 \mu\text{m}$ and density over 99% was obtained; neither the hardness nor fracture toughness were examined.

Alumina matrix composites containing 10 vol.% zirconia were manufactured by using filter and cold isostatic pressing methods for low temperature consolidation, and two-step sintering for a high temperature one [17]. It was proved that the low temperature consolidation technique has a negligible influence on the density and microstructure of the sinters when temperature T_1 is set at 1600°C .

In this paper, the two-step sintering of 2 and 12 vol.% nano-zirconia-alumina composite powders processed by filter pressing is reported. High-low and low-high schedules of heating temperatures were applied and compared to the constant heating rate schedule. The effects of the sintering schedule on the microstructure evolution and selected mechanical properties of the zirconia-alumina composite are studied.

EXPERIMENTAL PROCEDURE

Zirconia nano-powder of a mean particle size of 35 nm and globular crystallite shape was obtained by the hydrothermal crystallization of a precipitated hydrous zirconia gel under $\sim 3 \text{ MPa}$ for 8 h at 240°C in a 2 M NaCl solution. Zirconium oxychloride (purity > 99%, Si - 0.03%, Fe - 0.02%, Al. - 0.015%) and aqueous ammonia (analytically pure) were used for precipitation of the gel. High-purity alumina AKP-30 powder (Sumitomo Chemical Co., Japan) with no sintering additives was used.

A mixture of component powders composed of 90 vol.% AKP-30 and 10 vol.% zirconia (marked as ZTA) was prepared by attrition milling for 2 h using zirconia grinding media (3Y-TZP; 2 mm in diameter) in water acidulated by nitric acid to a pH of 2.5. Just before the end of milling, the pH value was increased up to 9 by using aqueous ammonia to induce a heteroflocculation effect. The flocculated slurry was filter pressed under 5.5 MPa (FP). The wet green compacts were dried to a constant weight in the presence of silica gel in

a desiccator. The samples of pure AKP-30 powder (called as AKP) were also prepared by using the milling and drying procedure described above. Preliminary experiments indicated a (2.0 ± 0.5) mass% debris of zirconia balls during milling. Therefore, the actual zirconia content in the ZTA and AKP samples was 12 vol.% and 2 vol.%, respectively.

The green ZTA and AKP compacts were sintered using the following temperature schedules: (i) 1350°C for 8 h, (ii) 1600°C for 2 h, (iii) 1600°C for 0 h followed by 1350°C for 8 h, and (iv) 1350°C for 8 h followed by 1600°C for 2 h. A heating rate of $10^\circ\text{C}/\text{min}$ and furnace cooling were applied between the soaking steps. Sintering schedules (i) and (ii) represent classical constant heating rate sintering (CHR); schedule (iii) refers to the two-stage sintering reported by Chen *et al.* [1] for nanocrystalline Y_2O_3 ceramics (TSS), and schedule (iv) follows Tartaj's approach [10] (RTSS). The sintering was preceded by dilatometry measurements to determine the sintering T_1 and T_2 temperatures for the two-step sintering. The measurements were performed in air using a DIL 402C (Netzsch) apparatus and a heating rate of $10^\circ\text{C}/\text{min}$.

The AKP-30 and nano-zirconia powders were characterised by using electron transmission microscopy (JEM-1011, Jeol) and the BET method (Nova 1200e, Quantachrome Inc).

The pore size distribution was measured by mercury porosimetry using a Quantachrome PoreMaster 60 apparatus. The density of the sintered bodies was determined by the Archimedes method. The microstructure of the samples was examined by SEM (FEI Nova 200 NanoSEM). The grain size was obtained by multiplying by 1.56 the average linear intercept length of at least 100 grains [1].

Both Vickers hardness and fracture toughness measurements were performed using a FV-700 Vickers Hardness Test apparatus. A load of 9.81 and 98.1 N were applied, respectively. The Palmqvist crack model was used for fracture toughness calculations [18].

RESULTS AND DISCUSSION

Powders and green compacts

The TEM images of the zirconia and alumina powders are shown in Figure 1. The AKP-30 powder has a particle size of $0.3 \div 0.5 \mu\text{m}$ and a BET surface area of $8.6 \text{ m}^2/\text{g}$ with an equivalent particle size $d_{\text{BET}} = 175 \text{ nm}$. The zirconia powder has a mean grain size of $\sim 10 \text{ nm}$ and surface area of $80 \text{ m}^2/\text{g}$.

The densities were $(52.6 \pm 0.5)\%$ and $(53.2 \pm 0.5)\%$ for the AKP and ZTA green samples, as calculated from the volume intruded data (Fig. 2). The pore sizes shifted towards smaller values due to the incorporation of nanometric zirconia crystallites into the space among larger alumina particles, as indicated by the pore size distribution curves shown in Figure 2.

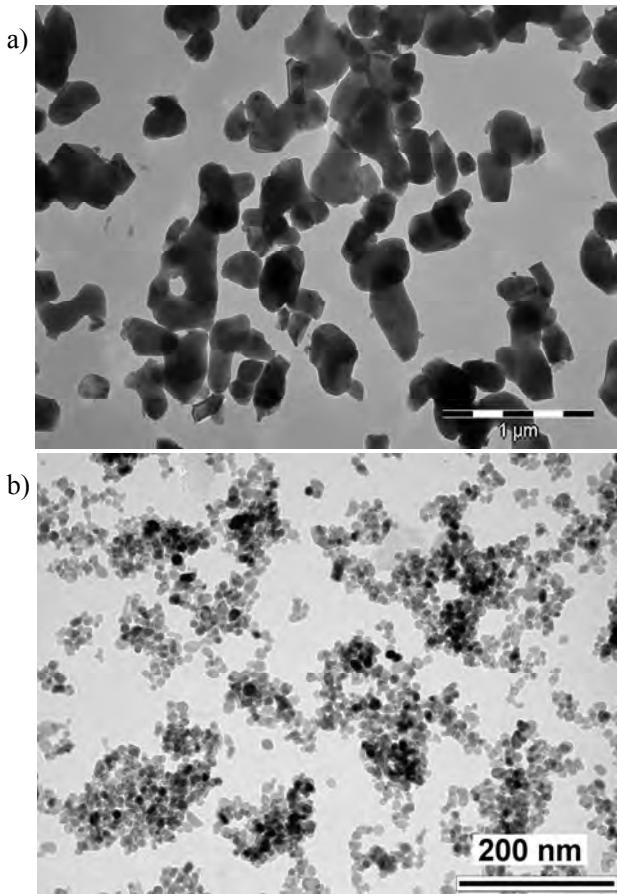


Fig. 1. TEM images of powders used: a) AKP-30, b) hydrothermal nano-zirconia

Rys. 1. Obrazy TEM użytych proszków: a) AKP-30, b) hydrotermalny nano-ZrO₂

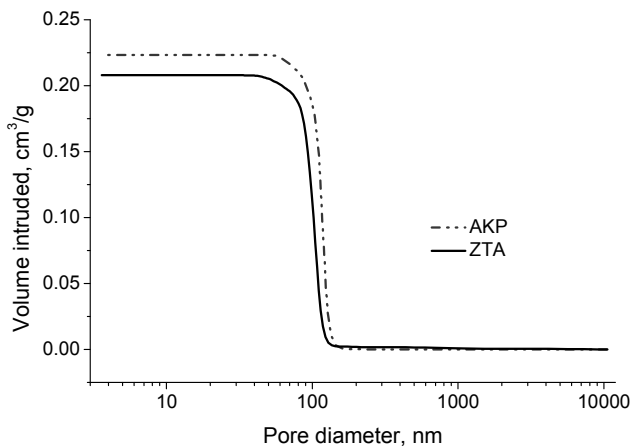


Fig. 2. Cumulative curves of pore size distribution of composite (ZTA) and alumina (AKP) filter pressed compacts

Rys. 2. Krzywe kumulacyjne rozkładu wielkości porów wyprasek z proszków kompozytowego (ZTA) i tlenku glinu (AKP) prasowanych filtracyjnie

Determination of sintering temperatures

Temperatures T_1 and T_2 strongly influence the results of two-step sintering [1]. Constant rate heating to temperature T_1 must yield a density of 75–90% during the first step of TSS. In this study, T_1 was chosen taking into consideration both literature data [16] and the

data of the densification rate (dp/dt) derived from the DIL experiment. The data shown in Figure 3 indicate a maximum densification rate of at about 1500°C for the ZTA sample (ZTA (1) curve). Hence, exhaustion of the densification rate is observed and attributed to the final sintering stage [19]. Moreover, the DIL curves show an insignificant influence of the zirconia additive on the sintering behaviour of the alumina powder (compare ZTA (1) and AKP), and some statistic effects concerning the reproducibility of the sample preparation (compare ZTA (1) and ZTA (2)). The densification rate curve of the ZTA sample in Figure 3 is shifted ~50°C towards higher temperatures when compared to the data reported by Wang *et al.* [16]. Relative density calculations based on the DIL data indicate the temperature of 1500°C being sufficient to obtain a density of about 75% and therefore being suitable as a minimum for the first step of TSS. However, to obtain greater densities, higher T_1 temperatures are required. Therefore a temperature of 1600°C was selected for the first step of sintering, accepting a risk originating from over-heating and corresponding grain growth.

The temperature of the second step of sintering also plays a very important role in TSS because a too low T_2 can exhaust the densification due to the suppression of atomic diffusion, but a too high T_2 can generate grain growth. For the second step of sintering, temperature T_2 was set at 1350°C, based on critical analysis of previous research reports [1, 8, 12, 16].

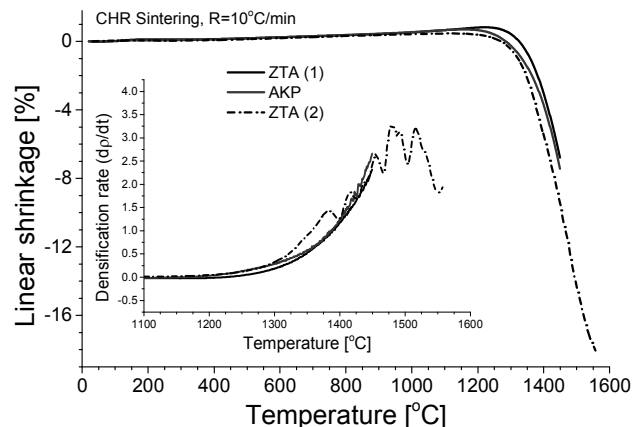


Fig. 3. Dilatometric curves of two ZTA samples and AKP sample filter pressed under 5.5 MPa. Inset shows related curves of densification rate as a function of temperature for constant-rate sintering (CHR)

Rys. 4. Krzywe dylatometryczne dwóch próbek ZTA i próbki AKP prasowanych filtracyjnie pod ciśnieniem 5,5 MPa. Wkładka pokazuje odpowiednie krzywe zależności szybkości zagęszczania w funkcji temperatury w przypadku spiekania przy stałej szybkości ogrzewania (CHR)

Microstructure and properties of sinters

The densities, microstructure and mechanical properties of the studied samples are shown in Table 1. The difference in density among the compacts sintered by using the CHR₂, TSS and RTSS schedules is insignificant, and the values of density are close to 95% in the

case of the ZTA samples and 99% in the case of the AKP samples they are moderate. This suggests that temperature T_1 was set too high, and the kinetics of grain boundary migration exceeded the kinetics of grain boundary diffusion, generating excessive grain growth, leading to a stable state of pores and, as a result, high porosity.

The above conclusion is confirmed by microstructural observations. The results shown in Figures 4-6 and in Table 1 indicate relatively large alumina grain sizes,

practically irrespective of the forming method applied, for low temperature consolidation of the composite powder. The grain growth ratios (final grain size divided by initial particle size of $0.2 \mu\text{m}$) for the ZTA samples are 12.5, 10.5 and 13.5, for the CHR₂, TSS and RTSS schedules respectively, and for the AKP samples they are 29, 19.5, 31. The advantageous microstructural result of TSS is observed both for the ZTA and AKP when compared to other heating schedules; the finest microstructure was obtained.

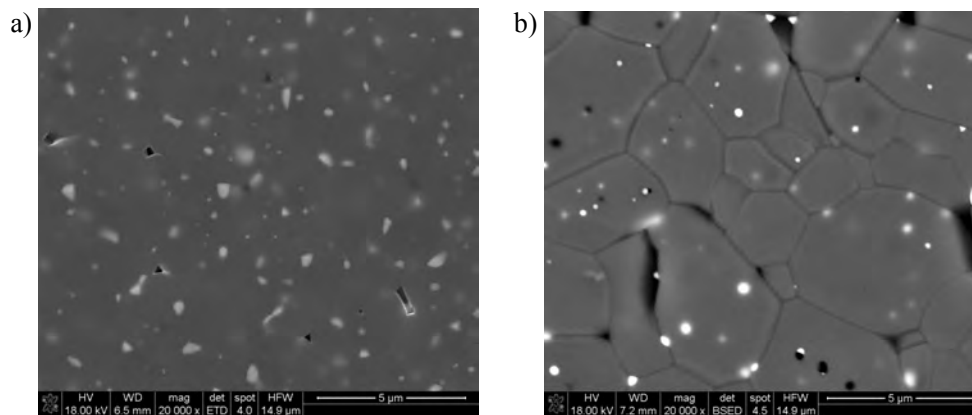


Fig. 4. SEM images of microstructure of compacts sintered for 8 h at 1350°C and additionally for 2 h at 1600°C (RTSS): a) ZTA, b) AKP; scale bar = $5 \mu\text{m}$

Rys. 4. Obrazy SEM mikrostruktury wyprasek spieczonych przez 8 h w 1350°C i dodatkowo przez 2 h w 1600°C : a) ZTA, b) AKP; znacznik powiększenia = $5 \mu\text{m}$

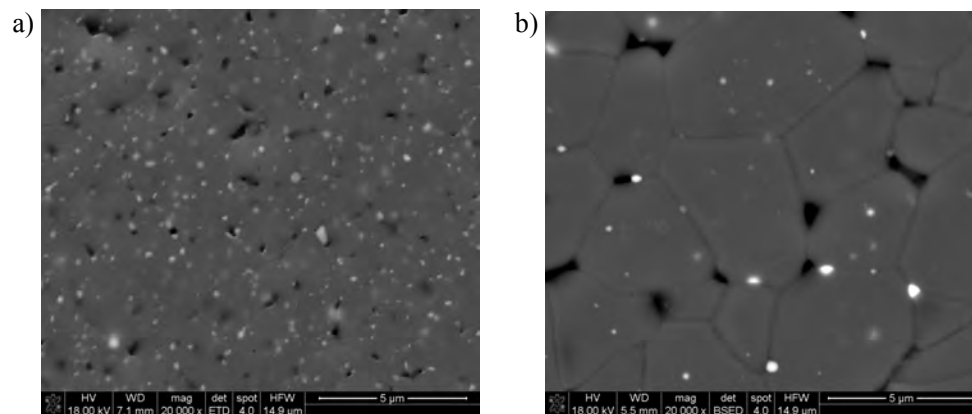


Fig. 5. SEM images of microstructure of compacts sintered for 0 h at 1600°C and additionally for 8 h at 1350°C (TSS): a) ZTA, b) AKP; scale bar = $5 \mu\text{m}$

Rys. 5. Obrazy SEM mikrostruktury wyprasek spieczonych przez 0 h w 1600°C i dodatkowo przez 8 h w 1350°C : a) ZTA, b) AKP; znacznik powiększenia = $5 \mu\text{m}$

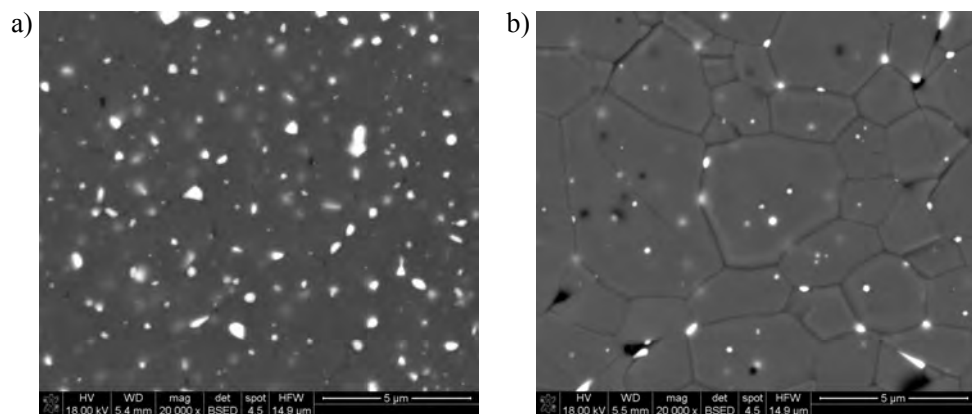


Fig. 6. SEM images of microstructures of samples sintered at 1600°C for 2 h (CRS): a) ZTA b) AKP; scale bar = $5 \mu\text{m}$

Rys. 6. Obrazy SEM mikrostruktur próbek spieczonych w 1600°C przez 2 h: a) ZTA, b) AKP; znacznik powiększenia = $5 \mu\text{m}$

TABLE 1. Relative density, grain size, Vickers hardness and fracture toughness of the sintered samples
 TABELA 1. Gęstość względna, rozmiar ziaren, twardość Vickersa i odporność na kruche pęknięcie K_{IC} spieczonych próbek

Schedule	Sample material	Sintering conditions	Relative density [%]	Grain size [μm]	H_V [GPa]	K_{IC} [$\text{MPa}\cdot\text{m}^{0.5}$]
CHR ₁	ZTA	1350°C/8h	71.57 ± 0.30	0.8±0.2	-	-
CHR ₂		1600°C/2h	95.80 ± 0.52	2.5±0.1	17.02 ± 0.24	5.93 ± 0.28
TSS		1600°C/0h+1350°C/8h	94.29 ± 0.34	2.1±0.1	20.83 ± 0.22	7.02 ± 0.12
RTSS		1350°C/8h+1600°C/2h	94.37 ± 0.16	2.7±0.1	16.13 ± 0.29	4.38 ± 0.11
CHR ₁	AKP	1350°C/8h	77.51 ± 0.47	1.2±0.2	-	-
CHR ₂		1600°C/2h	99.67 ± 0.28	5.8±0.1	16.68 ± 0.31	4.16 ± 0.16
TSS		1600°C/0h+1350°C/8h	98,16 ± 0,35	3.9±0.3	16.05±0.15	4.11±0.14
RTSS		1350°C/8h+1600°C/2h	99.29 ± 0.42	6.2±0.4	16.13 ± 0.29	4.18 ± 0.11

The SEM images shown in Figures 4-6 indicate that the zirconia grains are uniformly dispersed in the alumina matrix. The zirconia particles are located mainly in the grain boundaries or triple junctions of alumina. This proves the presence of the pinning effect, generating inhibition of alumina grain growth. However, some zirconia particles form intra-grain inclusions, indicating very the fast kinetics of grain-boundary migration at 1600°C, being the temperature T_I for TSS.

The influence of the heating schedule on the mechanical properties can be clearly seen in Table 1 as a result of the previously characterised features of the microstructure of composites, and additionally porosity and pore size distribution that were not studied in detail. The ZTA sample sintered by using the TSS schedule shows the highest values of both hardness and fracture toughness. It is worth remarking that reasonably good mechanical properties were obtained in the case of not fully densified materials.

CONCLUSIONS

Alumina matrix composites containing 2 vol.% and 12 vol.% zirconia were manufactured by using filter pressing (FP) and constant heating rate sintering (CHR), two-step sintering (TSS) or reverse two-step sintering (RTSS) for final temperature consolidation. The temperatures of 1350°C and 1600°C were selected to perform sintering.

There was an insignificant effect of the heating schedules on the densification of the composites, but it did have an impact on their microstructure. The ZTA composite containing alumina grains of ~2.4 μm and uniformly dispersed zirconia grains of ~0.25 μm was obtained in the case of the TSS schedule. The reversed two-step sintering (RTSS) led to the most coarse-grained microstructures, and is not recommended for the densification of ZTA composites using the studied heating schedule.

The temperature T_I of 1600°C generated large grain growth ratios during TSS, resulting in composites

showing densities close to 95%, but reasonably good hardness (20.8 ± 0.2 GPa) and fracture toughness ($7.0 \pm 0.2 \text{ MPa}\cdot\text{m}^{0.5}$) in the case of the ZTA composite.

Temperature T_I of the first step in two-step sintering should be set below 1600°C to obtain finer microstructures, larger densification and better properties of ZTA composites.

Acknowledgements

The work was financially supported by the European Union within the framework of the European Regional Development Fund under the Innovative Economy Operating Programme; grant no. POIG.01.03.01-00-024/08. The authors would like to thank Mrs. B. Trybalska, dr. P. Rutkowski and Mr. R. Lach for their assistance in SEM, DIL and BET/porosimetry measurements, respectively.

REFERENCES

- [1] Chen I.W., Wang X.H., Sintering dense nanocrystalline ceramics without final-stage grain growth, *Nature* 2000, 404, 168-171.
- [2] Maca K., Pouchly V., Zalud P., Two-step sintering of oxide ceramics with various crystal structures, *J. Eur. Ceram. Soc.* 2010, 30, 583-589.
- [3] Durán P., Capel F., Tartaj J., Moure C., A strategic two-stage low-temperature thermal processing leading to fully dense and fine-grained doped-ZnO varistors, *Adv. Mater.* 2002, 14, 2, 137-141.
- [4] Polotai A., Breece K., Dickey E., Randall C., Ragulya A., A novel approach to sintering nanocrystalline barium titanate ceramics, *J. Am. Ceram. Soc.* 2005, 88, 11, 3008-3012.
- [5] Wang X.H., Deng X.Y., Bai H.L., Zhou H., Qu W.G., Li L.T., Chen I.W., Two-step sintering of ceramics with constant grain-size. II. BaTiO₃ and Ni-Cu-Zn ferrite, *J. Am. Ceram. Soc.* 2006, 89, 2, 438-443.
- [6] Yu P.C., Li Q.F., Fuh J.Y.H., Li T., Lu L., Two-stage sintering of nanosized yttria stabilized zirconia processed by powder injection moulding, *J. Mater. Process. Tech.* 2007, 192-193, 312-318.

- [7] Binner J., Annapoorani K., Paul A., Santacruz I., Vaidyanathan B., Dense nanocrystalline zirconia by two stage conventional/hybrid microwave sintering, *J. Eur. Ceram. Soc.* 2007, 28, 5, 973-977.
- [8] Bodišová K., Šajgalík P., Galusek D., Švancárek P., Two-stage sintering of alumina with submicrometer grain size, *J. Am. Ceram. Soc.* 2007, 90, 1, 330-332.
- [9] Lee Y.I., Kim Y.W., Mitomo M., Effect of processing on densification of nanostructured SiC ceramics fabricated by two-step sintering, *J. Mater. Sci.* 2004, 39, 3801-3803.
- [10] Tartaj J., Two-stage sintering of nanosize pure zirconia, *J. Am. Ceram. Soc.* 2009, 92, S1, S103-S106.
- [11] Mazaheri M., Sintering of nanocrystalline zinc oxide via conventional sintering, *Two Step Sintering and Hot Pressing*, *Materiały Ceramiczne/Ceramic Materials* 2010, 62, 4, 506-509.
- [12] Ragulya A.V., Consolidation of ceramic nanopowders, *Advances in Applied Ceramics*, 107, 3, (2008), 118-134.
- [13] Lange F.F., Hirlinger M.M., Hindrance of grain growth in Al_2O_3 by ZrO_2 inclusions, *J. Am. Ceram. Soc.* 1984, 67(3), 164-168.
- [14] Raj R., Wang J., Activation energy for the sintering of two-phase alumina/ zirconia ceramics, *J. Am. Ceram. Soc.* 1991, 74 (8), 1959-1963.
- [15] Ye F., Liu L., Zhang J., Iwasa M., Su C.L., Synthesis of silicon nitride-barium aluminosilicate self-reinforced ceramic composite by a two-step pressureless sintering, *Comp. Sci. Tech.* 2005, 65, 2233-2239.
- [16] Wang Ch.J., Huang Ch.Y., Wu Y.Ch., Two step sintering of fine alumina-zirconia ceramics, *Ceram. Int.* 2009, 35, 4, 1467-1472.
- [17] Wójtowicz B., Pyda W., Two-step sintering and related properties of 10 vol.% ZrO_2 - Al_2O_3 composites derived from filter and cold isostatic pressing, *Materiały Ceramiczne* 2011, 4.
- [18] Niihara K., A fracture mechanics analysis of indentation-induced Palmqvist cracks in ceramics, *J. Mater. Lett.* 1983, 2, 221.
- [19] Hansen J.D., Rusin R.P., Teng M.H., Johnson D.L., Combined stage sintering model, *J. Am. Ceram. Soc.* 1992, 75, 5, 1129-1135.